Volume 27
Number 6
June 2025
Pages 1485–1732

Environmental Science
Processes & Impacts

rsc.li/espi

Themed issue: Indoor Environment

ISSN 2050-7887

ROYAL SOCIETY OF CHEMISTRY

PAPER
Ayomide A. Akande and Nadine Borduas-Dedekind
The gas phase ozonolysis and secondary OH production of cashmeran, a musk compound from fragrant volatile chemical products

Environmental Science Processes & Impacts

PAPER

View Article Online
View Journal | View Issue

Cite this: *Environ. Sci.: Processes Impacts*, 2025, **27**, 1504

The gas phase ozonolysis and secondary OH production of cashmeran, a musk compound from fragrant volatile chemical products†

Ayomide A. Akande and Nadine Borduas-Dedekind *

Fragrant personal care products are a subset of volatile chemical products (VCPs), an emerging source of outdoor pollutants capable of impacting air quality. Fragrant molecules, such as musks, are used in perfumes and have been found in aquatic organisms, water bodies, indoor air, and urban environments. Considering the distribution of musk-smelling compounds, there is a need to constrain their atmospheric fate indoors and outdoors. Here, we used a Vocus proton-transfer-reaction time-of-flight mass spectrometer to quantify the atmospheric oxidative fate of cashmeran, a bicyclic musk compound, detected in a commercial perfume alongside galaxolide, astratone and rosamusk. Cashmeran concentrations rose up to 0.35 ppbv representing a mass yield of 0.33 ± 0.04% of the perfume. We determined the second order rate constant of the cyclo-addition of O_3 with cashmeran to be (2.78 ± 0.31) × 10^{-19} cm^3 $molec^{-1}$ s^{-1} at 293 ± 1 K in N_2. This rate constant corresponds to an 85 day lifetime against 20 ppbv of O_3. Then, we repeated the ozonolysis experiments in air with 20% O_2 and measured significant secondary OH concentrations up to 5.1 × 10^5 molec cm^{-3}. Consequently, the lifetime of cashmeran in our experiment was shortened to 5 h. Thus, the oxidation of fragrant molecules, like cashmeran, could alter the oxidative capacity of indoor air *via* the production of secondary OH radicals. Furthermore, our results show that cashmeran is long-lived and could serve as a VCP tracer in urban air.

Received 26th July 2024
Accepted 12th October 2024

DOI: 10.1039/d4em00452c

rsc.li/espi

Environmental significance

Musk-smelling compounds, like cashmeran, are emitted from fragrant volatile chemical products. Using a Vocus mass spectrometer, we quantified the lifetime of cashmeran against 20 ppbv of O_3 to be 85 days. However, in the presence of O_2, cashmeran reacts with O_3 to produce secondary OH radicals up to 5.1 × 10^5 molec cm^{-3}, potentially influencing the oxidative capacity of indoor air.

1 Introduction

Volatile chemical products (VCPs), including personal care products, cleaning agents, paints, and pesticides, have been identified as an emerging source of anthropogenic volatile organic compounds (VOCs) in urban air.[1–3] These VOCs are precursors to ground-level O_3 and secondary organic aerosols (SOA), impacting air quality.[4–6] Additionally, VOCs can cause or aggravate respiratory diseases, headaches, and irritation of the eyes and nose.[7,8] To understand and predict the sources of VCPs to the atmosphere, specific VOCs have been identified as tracers for different VCP categories.[2] For example, D5-siloxane and limonene have been identified as reliable tracers for personal care products and fragrant VCPs, respectively.[2,9–11]

Synthetic musk compounds are a group of molecules synthesized specifically for their distinctive musky fragrance, commonly used in personal care products marketed for men.[12,13] These compounds are classified into four categories

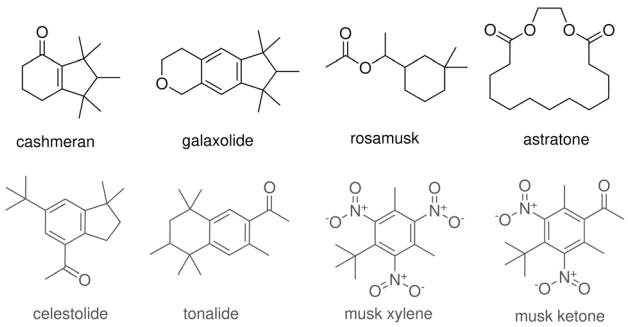

Fig. 1 Chemical structures of select synthetic musk compounds. Musk compounds detected in the commercial perfume used in this study are shown in black (top row), while other musk compounds reported in Table 1 are shown in grey (bottom row).

Department of Chemistry, University of British Columbia, Vancouver, Canada. E-mail: borduas@chem.ubc.ca; Tel: +1 604-822-4435

† Electronic supplementary information (ESI) available. See DOI: https://doi.org/10.1039/d4em00452c

Table 1 Reported literature on the presence and concentrations of synthetic musk compounds in various environments. Compounds with the highest concentrations in each study are shown here. Concentrations of nitro musks have also been included, where detected[a]

Molecule	Media	Description	*N*	Location	Concentration range (ref.)
Cashmeran	Air	Indoor air	20	Ontario, Canada	0.028–160 ng m^{-3} (ref. 15)
		Air from wastewater treatment plant	32	Ontario, Canada	n.d – 7.3 ng m^{-3} (ref. 15)
		Air from cosmetic plant	5	Taiwan	420–1000 ng m^{-3} (ref. 34)
		Air from women's sport centre	10	Izmir, Turkey	16.90 ± 6.7 ng m^{-3}, mean (ref. 31)
		Air from a primary school classroom	10	Izmir, Turkey	84.5 ± 35.2 ng m^{-3}, mean (ref. 31)
	Aquatic	Surface waters	10	Ontario, Canada	n.d – 0.71 ng L^{-1} (ref. 15)
		Wastewater treatment plants effluent	3	Ontario, Canada	76–9600 ng L^{-1} (ref. 15)
		Surface waters from rivers	34	Portugal	n.d – 104.4 ng L^{-1} (ref. 35)
		Carp fish species	13	Lake Chaohu, China	0.24–7.69 ng g^{-1} (dry weight) (ref. 13)
		Seafood	10	Tarragona, Spain	n.d – 11.2 ng g^{-1} (dry weight) (ref. 36)
		Sediment samples	12	Kadicha river, Lebanon	n.d – 94.22 ng g^{-1} (dry weight) (ref. 37)
	Human	Human blood	108	Vienna, Austria	n.d – 89 ng L^{-1}
Galaxolide	Air	Air from cosmetic plant	5	Taiwan	1000–1600 ng m^{-3} (ref. 34)
		Indoor air	20	Ontario, Canada	0.3–18 ng m^{-3} (ref. 15)
		Air from women's sport centre	10	Izmir, Turkey	144.0 ± 60.5 ng m^{-3}, mean (ref. 31)
		Air from a primary school classroom	10	Izmir, Turkey	267.3 ± 56.0 ng m^{-3}, mean(ref. 31)
		Outdoor air, summer	19	Ontario, Canada	n.d – 2.1 ng m^{-3} (ref. 15)
		Air from wastewater	10	Northern Germany	5.2–407.2 ng m^{-3} (ref. 24)
	Particulate matter	PM2.5 from women's sport centre	10	Izmir, Turkey	0.94 ± 0.52 ng m^{-3}, mean (ref. 31)
		PM2.5 from a primary school classroom	10	Izmir, Turkey	2.50 ± 0.94 ng m^{-3}, mean (ref. 31)
		Indoor dust	55	China	0.40–577 ng g^{-1} (ref. 32)
		House dust	10	Kumamoto, Japan	84–1600 ng g^{-1} (ref. 33)
	Aquatic	Seafood	10	Tarragona, Spain	17.1–367.3 ng g^{-1} (dry weight) (ref. 36)
		Carp fish species	13	Lake Chaohu, China	3.63–28.9 ng g^{-1} (dry weight) (ref. 13)
		Sediment samples	12	Kadicha river, Lebanon	n.d – 81.13 ng g^{-1} (dry weight) (ref. 37)
		Surface waters from rivers	34	Portugal	n.d – 379.2 ng L^{-1} (ref. 35)
		Surface waters	10	Ontario, Canada	n.d – 243 ng L^{-1} (ref. 15)
	Precipitation	Snow samples	42	Beijing, China	2.2–205.9 ng L^{-1} (ref. 30)
	Human	Human blood	108	Vienna, Austria	n.d – 6900 ng L^{-1}
		Human adipose	49	New York, USA	12–798 ng g^{-1} (lipid weight) (ref. 38)
		Human milk	54	Basel, Switzerland	55.02 ± 57.87 ng g^{-1} (lipid weight), mean (ref. 29)
Tonalide	Air	Air from cosmetic plant	5	Taiwan	610–960 ng m^{-3} (ref. 34)
		Indoor air	20	Ontario, Canada	0.09–17 ng m^{-3} (ref. 15)
		Air from women's sport centre	10	Izmir, Turkey	39.5 ± 14.7 ng m^{-3}, mean (ref. 31)
		Air from a primary school classroom	10	Izmir, Turkey	59.6 ± 13.5 ng m^{-3}, mean[31]
		Air from wastewater	10	Northern Germany	0.3–65.1 ng m^{-3} (ref. 24)
	Particulate matter	PM2.5 from women's sport centre	10	Izmir, Turkey	1.34 ± 0.71 ng m^{-3}, mean (ref. 31)
		PM2.5 from a primary school classroom	10	Izmir, Turkey	1.19 ± 0.37 ng m^{-3}, mean (ref. 31)
		Indoor dust	55	China	n.d – 120 ng g^{-1} (ref. 32)
		House dust	10	Kumamoto, Japan	n.d – 220 ng g^{-1} (ref. 33)
	Aquatic	Seafood	10	Tarragona, Spain	n.d – 16.0 ng g^{-1} (dry weight) (ref. 36)
		Carp fish species	13	Lake Chaohu, China	1.88–22.9 ng g^{-1} (dry weight) (ref. 13)
		Sediment samples	12	Kadicha river, Lebanon	n.d – 64.58 ng g^{-1} (dry weight) (ref. 37)
		Surface waters from rivers	34	Portugal	n.d – 60.6 ng L^{-1} (ref. 35)
		Surface waters	10	Ontario, Canada	n.d – 41 ng L^{-1} (ref. 15)
	Precipitation	Snow samples	42	Beijing, China	6.5–754.1 ng L^{-1} (ref. 30)
	Human	Human blood	108	Vienna, Austria	n.d – 290 ng L^{-1}
		Human adipose	49	New York, USA	8–134 ng g^{-1} (lipid weight) (ref. 38)
		Human milk	54	Basel, Switzerland	13.97 ± 9.96 ng g^{-1} (lipid weight), mean (ref. 29)
Astratone	Air	Air from wastewater	32	Ontario, Canada	n.d – 0.084 ng m^{-3} (ref. 15)
	Particulate	House dust	10	Kumamoto, Japan	n.d – 220 ng g^{-1} (ref. 33)
Celestolide	Air	Air from cosmetic plant	5	Taiwan	230–310 ng m^{-3} (ref. 34)
		Air from wastewater	10	Northern Germany	0.01–1.7 ng m^{-3} (ref. 24)
Musk Xylene	Air	Air from a primary school classroom	10	Izmir, Turkey	9.89 ± 2.76 ng m^{-3}, mean (ref. 31)
	Particulate matter	Indoor dust	55	China	n.d – 55.5 ng g^{-1} (ref. 32)
	Precipitation	Snow samples	42	Beijing, China	4.4–16.1 ng L^{-1} (ref. 30)
	Human	Human blood	152	Heidelberg, Germany	10–1183 ng L^{-1} (ref. 26)
		Human milk	54	Basel, Switzerland	2.93 ± 6.17 ng g^{-1} (lipid weight) (ref. 29)

Table 1 (*Contd.*)

Molecule	Media	Description	*N*	Location	Concentration range (ref.)
Musk Ketone	Particulate matter	Indoor dust	55	China	n.d – 203 ng g^{-1} (ref. 32)
		House dust	10	Kumamoto, Japan	n.d – 390 ng g^{-1} (ref. 33)
	Aquatic	Surface waters from rivers	34	Portugal	n.d – 78.2 ng L^{-1} (ref. 35)
	Precipitation	Snow samples	42	Beijing, China	6.7–43.2 ng L^{-1} (ref. 30)
	Human	Human blood	152	Heidelberg, Germany	10–518 ng L^{-1} (ref. 26)
		Human milk	54	Basel, Switzerland	1.60 ± 2.77 ng g^{-1} (lipid weight) (ref. 29)

[a] *N* is the number of samples and n.d refers to 'not detected'.

according to their structures: nitro-musks, polycyclic musks, macrocyclic musks, and alicyclic musks (see Fig. 1 for examples).[14] Due to their high molecular weights ranging from 206 to 297 g mol^{-1} (ref. 15) and their vapour pressures less than 71 Pa at 293 K, musk compounds can be classified as semi-volatile organic compounds.[16] There is growing interest in studying musk compounds because of their ubiquity in personal care products and their persistence in the environment.[17,18] For instance, ~4000 tons of polycyclic musks were used worldwide in 2000,[19] and they are emerging environmental contaminants.[20] Indeed, synthetic musk compounds have been detected in aquatic systems,[21–23] wastewater treatment plants,[15,24] aquatic organisms,[13,22] human blood,[25,26] human adipose tissue,[27] human breast milk,[28,29] outdoor air,[15] precipitation,[30] indoor air,[14,31] and indoor dust[32,33] (Table 1).

Cashmeran is a commonly used bicyclic musk and accumulates in aquatic organisms due to its lipophilic nature. A study on fifteen aquatic species from Lake Chaohu, China, found cashmeran to be present in 54% of the samples analyzed from the 15 aquatic species and to accumulate in the fishes' gills and livers preferentially.[13] Another study in Tarragona, Spain observed cashmeran in 3 out of 10 seafood species (Hake, Sole, and Cod) with concentrations of about 10 ng g^{-1}.[36] Furthermore, cashmeran was detected in 67%, 100%, 100%, and 88% of the 37 surface water samples taken from the Portuguese rivers: Ave, Leca, Antuã, and Cértima, respectively with concentrations up to 104.4 ng L^{-1}.[35] Additionally, cashmeran was the most abundant among five polycyclic musk compounds, galaxolide, cashmeran, celestolide, tonalide, and amberlan, detected in sediments collected along the Kadicha river basin in Lebanon, with concentrations up to 94.22 ng g^{-1} (Table 1).[37] Moreover, cashmeran poses a potential risk to the aquatic environment due to bioaccumulation.[39]

Cashmeran has a vapour pressure of 1 Pa at 25 °C,[40] and so cashmeran has also been detected in indoor air with offline techniques. Cashmeran was detected in air sampled from a primary school classroom and in window film samples collected from 10 offices in Turkey with average concentrations of 84.5 ± 35.2 ng m^{-3} and 18.3 ± 8.92 ng m^{-2} respectively.[14,31] It was also detected in all samples collected from 10 homes and 10 offices in Ontario, Canada with concentrations up to 160 ng m^{-3}.[15] Furthermore, nitromusks have been identified as endocrine disruptors, but exposure to cashmeran is unlikely to cause any estrogen, androgen, or thyroid modalities.[26,41] The detection of cashmeran in different environments indicates its emission from a range of fragrant products, including perfumes.

Here, we provide the first gas-phase real-time measurements of synthetic musk compounds from a commercial perfume using the Vocus proton-transfer-reaction time-of-flight mass spectrometer. We investigated the atmospheric ozonolysis of cashmeran which we identified as a major component of the perfume. We measured the lifetime of cashmeran under N_2 and in air to investigate the mechanism of OH radical and SOA production. Overall, we propose that cashmeran, and by extension other synthetic musk compounds, are long-lived atmospheric compounds and can be used as VCP tracers for fragrant products.

2 Methods

2.1 Chemicals

A leading brand of a musk-smelling commercial perfume marketed for men was purchased from Amazon, Canada, and used here. Cashmeran (96%) was obtained from Toronto Research Chemicals. 1,3,5-Trimethylbenzene (98%), cyclohexane (99.9%) and acetonitrile (HPLC Plus, ≥99.9%) were purchased from Sigma-Aldrich and used without further purification. A solution of 350 mM of cashmeran was prepared by dissolving the solid in a 70 : 30 mixture of ultrapure Milli-Q water (resistivity of >18.2 MΩ cm, PURELAB Option Q-7 system) and acetonitrile. An organic solvent was necessary to dissolve cashmeran and acetonitrile was chosen for its low *m*/*z* ratio and lower sensitivity on the Vocus.

2.2 Experimental setup

Experiments were carried out in a dark 8 m^3 Teflon smog chamber (Ingeniven LLC) covered by black-out curtains (see Fig. S1 and S2†).[42] 1/4″ OD fluorinated ethylene propylene (FEP)[43,44] (Cole-Parmer LLC) tubing was used to connect the instruments to the middle of the chamber *via* stainless steel gaugeable 1/4 in. fittings (Swagelok). The instruments pulled a total of 9 L min^{-1} from the chamber during each experiment.

Either N_2 or particle-free air was used in this study. The particle-free air was supplied from an oil-less air compressor and passed through a particle filter, a water separator, and a dryer unit. For additional particle filtration, two particle filter cartridges (Parker Balston) were placed in line. To generate N_2, the particle-free air was fed into a nitro pack generator (Parker

Balston, Model 76-97) which removes O_2, CO_2, hydrocarbons, and particles from 0.01 microns.

To clean between experiments, 400–900 ppbv of excess O_3 was left in the bag for an additional 12 h in batch mode to drive complete oxidation of any remaining VOCs. The chamber was then emptied at a flow of 20 L min^{-1}, and because of a pulley system, the chamber was able to be completely deflated. Next, the chamber was refilled with N_2 or particle-free air, and continuously purged for 24 h. After this cleaning procedure, the Vocus and a scanning mobility particle sizer (SMPS) were used to confirm that background signals of cashmeran and particles had been reached before the start of an experiment. To deep clean the smog chamber and to remove any accumulated organic matter on the walls, we pressure washed (Echo, MS-21H) the chamber with Milli-Q water and dried the chamber by purging with compressed air at 20 L min^{-1} for 72 h.

2.3 Instrumentation

2.3.1 Vocus 2R PTR-ToF-MS. The proton-transfer-reaction time-of-flight mass spectrometer (PTR-ToF-MS, Vocus 2R (Tofwerk AG/Aerodyne Research, Inc.)[45] was used to identify the musk compounds reported in this study as well as follow their kinetics and products of oxidation. The Vocus has a mass resolving power of $m/\Delta m$ > 10 000 and uses hydronium ions (H_3O^+), generated *via* a plasma discharge method, as its reagent ion.[45,46] The Vocus was operated under optimized conditions with a drift pressure of 2.1 mbar, an ion source voltage of 427 V, an ion source current of 2 mA, an E/N ratio of 131 Td, a reagent ion flow rate of 20 sccm, and a molecular reactor temperature of 60 °C. The Vocus pulled at 6 L min^{-1} from the chamber, with 100 sccm subsampled into the instrument's focusing ion molecular reactor (FIMR). Mass spectra were recorded from 7 to 406 m/z with a single ion signal of 2.70 mV × ns and 1 Hz time resolution. A polytetrafluoroethylene (PTFE) filter (Savillex) was placed in front of the Vocus inlet to ensure that only gas-phase molecules were being sampled during the kinetics experiments. Data obtained were processed using either Tofware (Aerodyne/Tofwerk) v3.2.5 within Igor (Wavemetrics) Pro v8 or Tofware v3.3.0 within Igor Pro v9.

2.3.2 Scanning mobility particle sizer. A scanning mobility particle sizer (SMPS, Model 3938, TSI Inc., Shoreview, MN) was used to quantify the number and size distribution of particles. The SMPS operated with a total scan time of 1 min and measured particle sizes ranging from 10–300 nm in diameter. The SMPS sampled at a flow rate of 1 L min^{-1} and a sheath air flow rate of 10 L min^{-1} with an inlet impactor of 0.071 cm. Data acquired by the SMPS was processed using Matlab (MathWorks).

2.3.3 O_3 generator and trace gas analyzers. O_3 was generated by passing a flow of 1 L min^{-1} of particle-free air through a UV lamp O_3 generator (Jetlight Company, Model 610). The concentration of O_3 was monitored with an O_3 analyzer (either iQ Series 49, Thermo Scientific, or Model 205 Dual Beam, 2B Technologies) with a time resolution of 1 min. In addition, a 42iQ NO–NO_2–NO_x analyzer (Thermo Scientific) was used to ensure there were no nitrogen oxides (NO, NO_2, NO_x) in the chamber.

2.3.4 GC-MS for confirmation of cashmeran in perfume. To independently confirm the identity of cashmeran within the commercial perfume, we used a separate gas chromatograph coupled to a mass spectrometer (GC-MS) (Model 5957B, Agilent Technologies). The GC-MS operated with a standard HP-5ms column: 30 m long with an inner diameter of 0.25 mm and 0.25 μm film thickness. The oven temperature was initially ramped at 20 °C min^{-1} for 7 min, then 5 °C min^{-1} for 16 min, and finally at 25 °C min^{-1} for 5 min. The oven's initial and final temperatures were 20 °C and 280 °C respectively, with a total GC runtime of 28 min. Cashmeran (m/z 206.2) eluted at 11.6 min (see Fig. S3†).

2.3.5 UV/vis spectrometer. To determine the absorption spectra of cashmeran, we measured the absorbance of the dissolved cashmeran (350 mM) in a water : acetonitrile (70 : 30) solution with a double-beam UV/vis spectrophotometer (Carry-5000, Agilent). The measurements were baseline corrected using a solution of water:acetonitrile (70 : 30).

2.4 Analysis of musk-smelling compounds in perfume

2.4.1 Calibration of musk compounds. Volumes ranging from 2 to 10 μL of a commercial perfume were injected into the 8 m^3 dark chamber using a syringe, through a gently heated U-shaped glass tube with N_2. The compounds were monitored by the Vocus and the particles by the SMPS. The Vocus signal at m/z 207.1743 ($C_{14}H_{23}O^+$) was calibrated for cashmeran by injecting known concentrations of the commercially pure compound into the chamber with a glass syringe *via* a U-shaped glass tube and using a heat gun (see Fig. S2 and S4†). The injections were done every 10 min with N_2.

The obtained sensitivity of 4115 cps ppb^{-1} for cashmeran (Fig. S4†) was then applied to galoxolide, rosamusk and astratone (Fig. 1). We acknowledge that applying the obtained sensitivity of cashmeran to the other musk compounds is an approximation considering their different functional groups, potential fragmentation, molecular weight, and the transmission efficiency posed by PTR-MS.[47,48]

2.4.2 Mass yield in perfume analysis. Next, we quantified the mass yield of the musk compounds in the perfume across three experiments. First, the perfume's total mass was calculated using its density of 0.83 g cm^{-3}, and volume injected (2 to 10 μL) during each experiment. The mass of the four identified musk compounds was then obtained from their estimated mixing ratios and divided by the perfume's total mass to get the mass yields. (see S8 and Table S2†).

2.5 Ozonolysis of cashmeran

2.5.1 Chemical kinetics. During a typical ozonolysis experiment, the pre-cleaned chamber was first filled with N_2 or particle-free air (depending on whether secondary OH radical production was being suppressed or studied, respectively). Pure cyclohexane (0.33 ppmv) was added to study secondary OH radical production as it is a known OH probe.[49] Next, 10–15 μL of a 350 mM cashmeran solution dissolved in water :

acetonitrile (70 : 30) was introduced into the chamber with a syringe *via* either the U-shaped glass tube or a 3-neck round bottom flask, and heated gently with a heat gun with a flow of N_2 (see Fig. S2†). When the signal of cashmeran steadied after 1 hour, excess O_3 between 400 and 1000 ppbv was introduced into the chamber, and the reaction was allowed to proceed in batch mode (Fig. S8†). O_3 was typically added over a period of 1 to 1.5 h before the O_3 generator was stopped, ensuring a large excess of O_3 compared to the analyte for pseudo-first order kinetics. The large O_3 excess was necessary (1) to operate under pseudo-first order reaction kinetics, and (2) to accelerate the reaction rate to reasonable experimental times (less than 18 h).

The change in concentration of cashmeran due to reactions with O_3 and OH radicals is given by eqn (1). The integrated rate law is given by eqn (2).

$$-\frac{d[C_{14}H_{22}O]}{dt} = k_{O_3}[O_3][C_{14}H_{22}O] + k_{OH}[OH]_{ss}[C_{14}H_{22}O] \quad (1)$$

$$\ln\frac{[C_{14}H_{22}O]_t}{[C_{14}H_{22}O]_0} = -\left(k_{O_3}[O_3] + k_{OH}[OH]_{ss}\right)t \quad (2)$$

where $[C_{14}H_{22}O]_t$ is cashmeran's signal at time t, $[C_{14}H_{22}O]_0$ is cashmeran's signal at time 0 s, k_{O_3} and k_{OH} are the second order rate constants of cashmeran with O_3 and OH radicals, respectively, in cm^3 $molec^{-1}$ s^{-1}, $[O_3]$ is the average concentration of O_3 in molec cm^{-3}, $[OH_{ss}]$ is the steady-state concentration of OH radicals in molec cm^{-3}, and t is the time in seconds.

The rate constant, k_{O_3}, of cashmeran with O_3 was determined from experiments strictly under N_2, to prevent OH radical production and to simplify eqn (2). The experiments were conducted in triplicate at temperatures of 292 K and 293 K (Fig. 3).

2.5.2 Quantification of OH radical concentrations

2.5.2.1 Predicted rate constant of cashmeran with OH radicals from a structure–activity relationship model. The integrated rate law, eqn (2), was used to estimate the production of secondary OH radicals during the experiments in air. Cashmeran's rate constant with OH radicals, k_{OH}, was theoretically predicted using the Atmospheric Oxidation Program for Microsoft Windows (AOPWIN) from the United States Environmental Protection Agency Estimations Program Interface suite (EPI-WEB 4.1).[50] AOPWIN employs structural–activity relationships to estimate gas-phase rate constants between organic molecules and common oxidants such as O_3 and OH radicals[50] (see S9†). The ozonolysis experiments in the presence of O_2, were carried out between 290 and 295 K. Since the rate constant is temperature-dependent according to the Arrhenius equation, there is an additional uncertainty in our reported concentrations, but one that would fall within the standard deviation of our reported rate constants.

2.5.2.2 Estimated OH radical production using TMB as a probe. In addition, 0.4 pptv of 1,3,5-trimethylbenzene (TMB) was introduced to an experiment conducted in particle-free air to estimate the concentration of secondary OH radicals produced.[51,52] TMB reacts slowly with O_3 (k(1,3,5-trimethylbenzene + O_3) = 2.20×10^{-21} cm^3 $molec^{-1}$ s^{-1})[53,54]), but rapidly with OH radicals (k(1,3,5-trimethylbenzene + OH radicals) = 5.53×10^{-11} cm^3 $molec^{-1}$ s^{-1}).[52] Therefore, its decrease in concentration can be attributed solely to reactions with OH radicals.[55] Finally, attempts at measuring the OH radical rate constant with cashmeran using TMB and the relative rate method were complicated by photolysis chemistry (Fig. S16†) and particle production, and so we opted to estimate OH radicals *via* AOPWIN.

2.5.3 Wall loss experiment. Cashmeran was observed to be steady in the chamber beyond 8 h (Fig. S5†). Additionally, we ran a purging experiment at 14 L min^{-1} and found cashmeran to follow the theoretically determined first-order rate decay. Both observations indicate minimal wall chemistry participation for the duration of the ozonolysis kinetics experiments (Fig. S6 and Table S1†).

2.5.4 Minimizing SOA formation. Secondary organic aerosol (SOA) formation was monitored by the SMPS and observed during ozonolysis of cashmeran in particle-free air only (not in N_2). The SOA in particle-free air was due to the presence of cashmeran since no aerosol formation was observed in the presence of cyclohexane and O_3 (Fig. S10†). To minimize the production of SOA and the addition of a partitioning sink for cashmeran, we used an average of (0.30 ± 0.13) ppbv cashmeran throughout our experiments in air.

3 Results and discussion

3.1 Cashmeran detected in a commercial perfume

First, we analyzed a commercial musk-smelling perfume with the Vocus to identify the emitted VOCs. We identified four structurally different musk compounds: cashmeran at m/z 207.1743, galaxolide at m/z 259.2056, astratone at m/z 271.1904, and rosamusk at m/z 199.1693 (Fig. 1 and 2). Cashmeran was

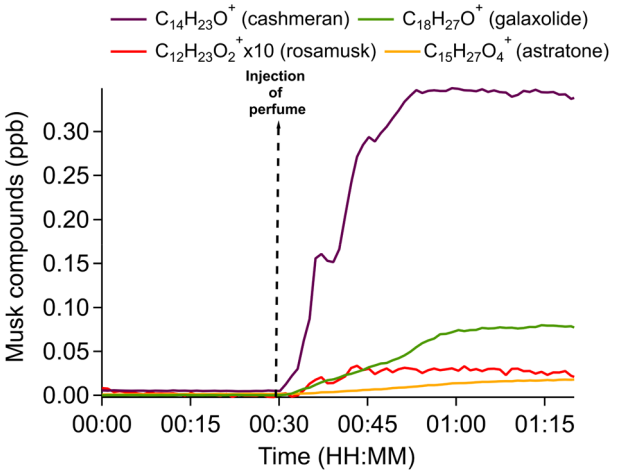

Fig. 2 The time series of musk compounds following the injection of 10 μl of perfume into the 8 m^3 smog chamber was measured by the Vocus. Cashmeran, galaxolide, astratone, and rosamusk were identified in the commercial perfume. We used the sensitivity of cashmeran at m/z 207.1743 (4115 cps ppb^{-1}) to convert the Vocus signals of galaxolide m/z 259.2056, astratone (m/z 271.1904), and rosamusk (m/z 199.1693) into mixing ratios. Note that the concentration of rosamusk was multiplied by a factor of 10 for scaling.

the most prominent musk compound detected by the Vocus with a calibrated signal of up to 0.35 ppbv (Fig. 2). Since the Vocus only provides molecular formula information, we needed to confirm that the signal at m/z 207.1743 and the chemical formula $C_{14}H_{23}O^+$ corresponded to cashmeran. To do so, we injected the commercial perfume into a GC-MS and matched the retention time on the GC to an internal standard of cashmeran (Fig. S3†). Furthermore, the fragmentation patterns of cashmeran in the perfume and the cashmeran standard were identical (Fig. S3†). We therefore confirmed the presence of cashmeran in the fragrance.

Next, cashmeran's sensitivity (Fig. S4†) was applied to galaxolide, astratone and rosamusk, resulting in concentrations of up to 0.07 ppb, 0.01 ppb, and 0.003 ppb, respectively. Moreover, we determined the mass yield of each musk compound in the perfume (in triplicate, Fig. S7†). We report the mass yield of cashmeran, galaxolide, astratone, and rosamusk to be (0.33 ± 0.04)%, (0.08 ± 0.03)%, (0.02 ± 0.01)%, and (0.003 ± 0.001)% respectively (Table S2†). Together, these musk compounds account for ~0.43% of the perfume's mass, with cashmeran as the dominant compound by an order of magnitude.

For comparison, the observed concentration of cashmeran in the musk-smelling commercial perfume was 45 times higher than concentrations measured in air sampled from homes and offices, where levels reached up to 160 ng m^{-3} (Table 1).[15] The higher concentrations reported in our study are consistent with our experiments capturing the emissions directly from the perfume. The fragrant component of personal care products is an important source of VOCs indoors, yet product labels do not include fragrant VOC emissions.[56]

3.2 Ozonolysis of cashmeran

3.2.1 Chemical kinetics under N_2. Since cashmeran was the dominant musk compound in the perfume observed by the Vocus, we focused on its chemical kinetics to gain insights into its atmospheric fate. First, we introduced cashmeran and then an excess of O_3 into our 8 m^3 smog chamber prefilled with N_2, and monitored its decay with the Vocus (Figure S8†). Of note, the kinetic experiments were conducted under N_2 to precisely measure the rate constant of the initial [4 + 2] cyclo-addition reaction of O_3 to cashmeran's C–C double bond. This step is rate-limiting.[57,58] We determined a rate constant of (2.78 ± 0.31) × 10^{-19} cm^3 $molec^{-1}$ s^{-1} at a temperature of 293 ± 1 K under dry conditions (RH < 10%) in triplicate experiments (Fig. 3). This rate constant obtained in N_2 translates to a lifetime of 211 days against 8 ppbv of O_3, the average O_3 concentration observed indoors during field campaigns HOMEChem[59] and CASA.[60] The lifetime of cashmeran drops to 85 days against 20 ppbv of O_3, which is the Canadian maximum long-term exposure limit of O_3 indoors over 8 h.[61] Clearly, cashmeran has a long atmospheric lifetime against O_3.

Additionally, we compared the ozonolysis rate constant obtained here with the estimated output from AOPWIN/US EPA EPI Suite, a quantitative structure–activity relationship model.[50] The model estimates the rate constant of cashmeran with O_3 to be 1.14 × 10^{-17} cm^3 $molec^{-1}$ s^{-1} at 298 K, which is two orders of magnitude faster than our reported rate constant, (2.78 ± 0.31) × 10^{-19} cm^3 $molec^{-1}$ s^{-1} in N_2. This overestimation is likely due to the electron-deficient moiety of the α,β-unsaturated ketone that is not accurately accounted for in the predicted calculation. The carbonyl group in cashmeran pulls electron density away from the R–C=C–R through a mesomeric effect, causing the C–C double bond to be less nucleophilic than a C–C double bond in a saturated molecule. This 2-order of magnitude overestimation by EPI Suite could be corrected by accounting for substituents on the C=C moiety.

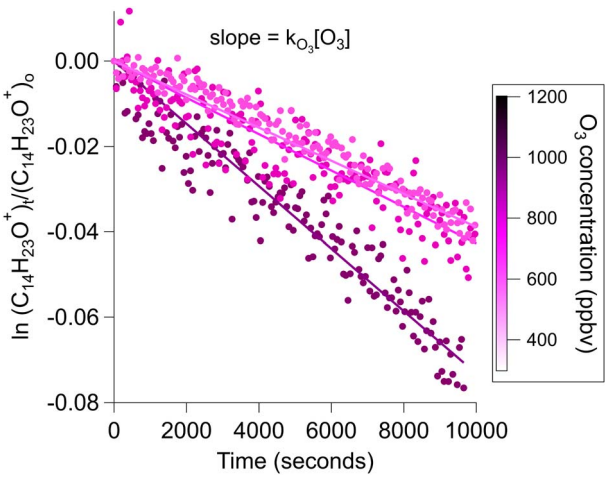

Fig. 3 The kinetics traces of cashmeran as a function of time are colour-coded by the O_3 concentration. The data was pre-averaged by 1 minute intervals. The rate constant was determined to be (2.78 ± 0.31) × 10^{-19} cm^3 $molec^{-1}$ s^{-1}. No wall loss corrections were necessary for the 8000 L chamber (see Fig. S5†). The rate constant was calculated by dividing the slope by the concentration of O_3.

3.2.2 Production of secondary OH radicals from cashmeran's oxidation with O_3. Next, we looked at the fate of cashmeran under atmospherically relevant conditions by repeating the ozonolysis experiments in particle-free air in the presence of O_2. Several alkenes, including 1,3-butadiene, α-pinene, isoprene, cyclohexene and 2,3-dimethyl-2-butene, have been shown to generate OH radicals as a secondary byproduct during ozonolysis.[57,62–64] The yields of OH radicals ranged from 0.08 for 1,3-butadiene to 1.00 for 2,3-dimethyl-2-butene.[58] Given that cashmeran is a bicyclic alkene, we hypothesized that it also had the potential to generate OH radicals as a secondary product.

To assess the formation of OH radicals in the chamber, we added cyclohexane as an OH radical probe,[49] despite the fact that cyclohexane is not detected by the Vocus. Instead, we monitored with the Vocus the production of $C_6H_{11}O^+$, most likely cyclohexanone, a known oxidation product of cyclohexane and OH radicals.[65] Cyclohexanone increased with signals up to 1.2 × 10^4 counts s^{-1} in all experiments under air (Fig. 4). Next, we carried out a control experiment without cashmeran to verify that OH radical production originated from the ozonolysis of cashmeran. Indeed, no cyclexanone was observed without cashmeran nor in the absence of O_2 (Fig. 4). Thus, cashmeran and likely other large alkenes used in fragrances, can produce OH radicals and so the next step was to quantify the amount of OH radicals produced.

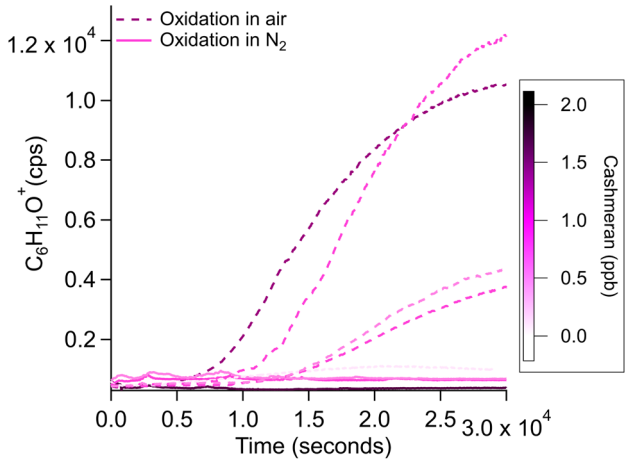

Fig. 4 The production of $C_6H_{11}O^+$ (*m*/*z* 99.0804), cyclohexanone, was measured during ozonolysis experiments in air and in N_2 to monitor the production of secondary OH radicals. Cyclohexanone was produced only in experiments in air, indicating the role of O_2 in secondary OH chemistry. The ozonolysis experiments were carried out at varying concentrations of cashmeran and each trace is colour-coded with the concentration of cashmeran used.

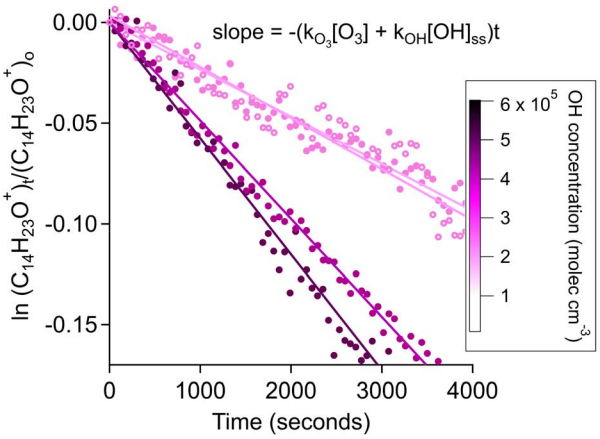

Fig. 5 The decay slope of cashmeran is plotted as a function of time during ozonolysis in the presence of O_2. The markers and linear fit are colour-coded with the estimated concentration of OH radicals produced within each reaction (Table 2). Four experiments are plotted and runs 3 & 4 are distinguished by open and filled markers. All data was pre-averaged by 1 minute interval.

3.2.3 Estimation of secondary OH radicals produced

3.2.3.1 Estimating OH radical production from estimating k_{OH}. Considering the relatively long lifetime of cashmeran with O_3 and its ability to produce OH radicals as a secondary product, we sought to quantify the relative contribution of each oxidant to the fate of cashmeran. We determined the OH radicals concentration from the integrated rate law of cashmeran reacting with both O_3 and OH radicals (eqn (2)). To make this calculation, we used the theoretical rate constant output from the US EPA EPI Suite estimation model, k_{OH}, $= 1.08 \times 10^{-10}$ cm^3 $molec^{-1}$ s^{-1} and our measured O_3 rate constant, k_{O_3}, $= 2.78 \times 10^{-19}$ cm^3 $molec^{-1}$ s^{-1}. Using eqn (2), we calculated the steady-state concentration of OH radicals in our triplicate experiments in the presence of O_2 (Table 2). The average concentration of OH radicals produced was $(3.29 \pm 1.60) \times 10^5$ molec cm^{-3} (Fig. 5 and Table 2). This value is comparable with indoor steady-state indoor OH concentration such as 1.7×10^5 molec cm^{-3} predicted in indoor air,[66] and measured up to 1.8×10^6 molec cm^{-3} in a classroom.[67] While ozonolysis reaction can occur solely *via* the addition of O_3 to cashmeran's C–C double bond, reactions with OH can proceed *via* two pathways: the addition of OH to the C–C double bond and the abstraction of a hydrogen atom.[68–70] Thus, the reaction of cashmeran with OH radicals is less affected by the electron-deficient moiety of the α,β-unsaturated ketone compared to its reaction with O_3. This rationale supports our use of the US EPA EPI Suite estimated rate constant of cashmeran's reaction with OH radicals despite the model's overestimation of the compound's rate constant with O_3.

Table 2 Estimated OH radicals concentration from experiments in particle-free air. The experimentally determined rate constant of cashmeran with O_3, 2.78×10^{-19} cm^3 $molec^{-1}$ s^{-1}, and the theoretical rate constant of cashmeran with OH radicals, 1.08×10^{-10} cm^3 $molec^{-1}$ s^{-1}, were used to make these calculations

Experimental runs	O_3 concentration (molec cm^{-3})	Estimated OH radicals concentration (molec cm^{-3})
1	9.75×10^{12}	4.25×10^5
2	1.06×10^{13}	5.05×10^5
3	1.14×10^{13}	1.87×10^5
4	1.10×10^{13}	1.99×10^5

3.2.3.2 Estimating OH radical production using TMB as a probe. To further constrain this calculated OH radical concentration, we measured the concentration of OH radicals by monitoring the decay of a reference compound, 1,3,5-trimethylbenzene which has a well constrained rate constant with OH radicals of 5.53×10^{-11} cm^3 $molec^{-1}$ s^{-1} (Fig. S11 and S12†).[52] We estimated the steady-state concentration of OH radicals produced to be 1.58×10^5 molec cm^{-3}.[52] TMB was chosen as the reference compound since its reaction with O_3 to form secondary OH will not compete with the ozonolysis of cashmeran; indeed TMB's rate constant with O_3 is 2 orders of magnitude slower at 2.20×10^{-21} cm^3 $molec^{-1}$ s^{-1}.[53,54] Nevertheless, we recognize that TMB could react with secondary OH from cashmeran ozonolysis, generating more OH radicals and increasing the overall OH concentration. Therefore, the reported OH concentrations are an upper bound.

3.2.3.3 Overall secondary OH radical production. The agreement between the calculated value using k_{OH} from EPI suite, $(3.29 \pm 1.60) \times 10^5$ molec cm^{-3}, and the TMB experimental method, 1.58×10^5 molec cm^{-3}, suggests that the expected secondary OH radical production is indeed on the order of 10^5 molec cm^{-3} during ozonolysis of cashmeran.

We calculated the OH molar yield (similar to eqn (S1)†) from the ozonolysis of cashmeran to be 0.004%, assuming the lowest

estimate of one OH radical produced per cashmeran molecule. Although this yield is small, it increases the decay rate of cashmeran in air by an order of magnitude compared to in N_2, indicating that OH radicals govern the atmospheric fate of cashmeran (Fig. S8†).

3.3 Oxidation products

3.3.1 Gas phase. We detected the formation of $C_{14}H_{23}O_2^+$ as the key oxidation product during ozonolysis in both air and N_2 (Fig. 6 and S14†). We confirmed that this product was in the gas phase by having a PTFE filter in front of the inlet throughout all our measurements. This chemical formula suggests that the oxidation product is cashmeran with one additional oxygen atom. The linear correlation between cashmeran and $C_{14}H_{23}O_2^+$ indicates that this product is likely a first-generation product (Fig. 6). The signal of $C_{14}H_{22}O_2$ was quantified using the calibration factor of cashmeran (4115 cps ppb^{-1}) (Fig. S4†). Based on the sensitivity of cashmeran, we calculated the yield of the ozonolysis product, $C_{14}H_{22}O_2$ to be 13%.

During ozonolysis of alkenes, the electrophilic O_3 molecule attacks the C=C bond and undergoes a cyclo-addition forming the primary ozonide.[71,72] The ozonide is an transient molecule with excess internal energy and quickly dissociates by breaking the O–O–O bond. This dissociation leads to the formation of the criegee intermediate, which can rearrange as well as act as an oxidant.[73] We propose that the $C_{14}H_{23}O_2^+$ product is likely an epoxide *via* a dioxolane intermediate (see Fig. S13† for proposed structure).[74]

We observed the trace of $C_{14}H_{23}O_2^+$ in the absence of cashmeran to determine whether it was being formed as an artifact (see Fig. S15†). While there was a slight increase in its signal, it was quickly removed at approximately 50 ppbv of O_3. Thus, we conclude that this artifact does not significantly affect the quantification of the oxidation product detected at the same *m*/*z*. However, we acknowledge that the oxidation product ($C_{14}H_{23}O_2^+$) may fragment into cashmeran in the Vocus. If this fragmentation occurs, it implies that our reported rate is slightly lower than the true ozonolysis rate constant, indicating that we are providing a lower bound for the rate constant.

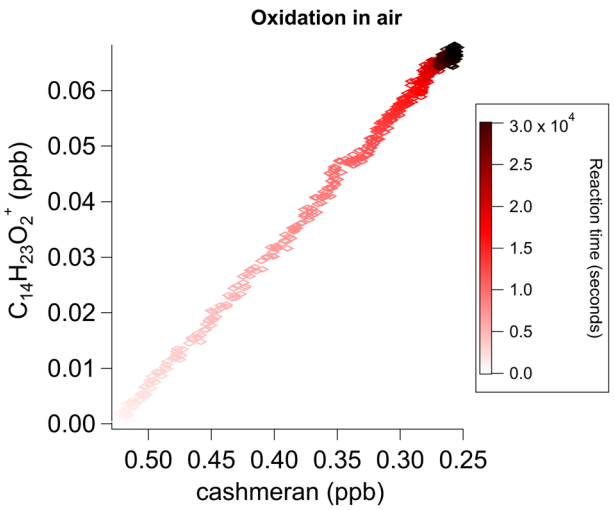

Fig. 6 The evolution of $C_{14}H_{22}O_2$ over time during the ozonolysis of cashmeran in air follows a linear correlation indicative of a first-generation product. The same plot was obtained under N_2 (Fig. S14†).

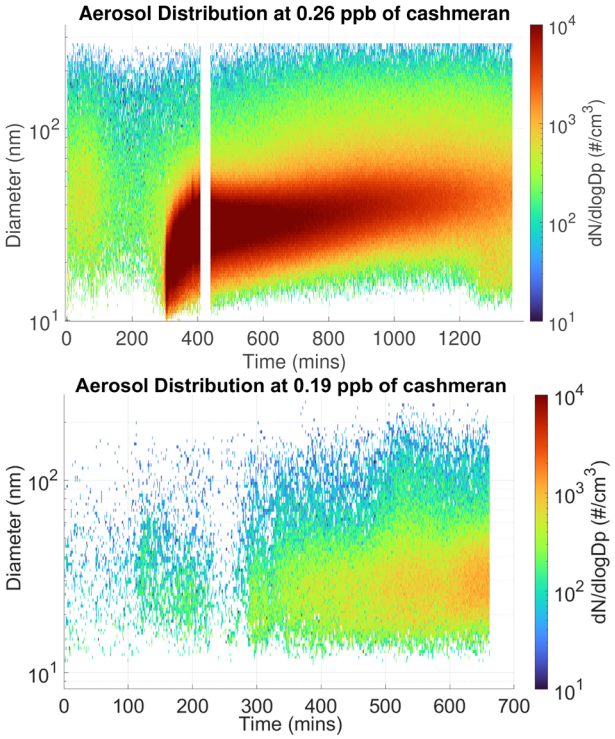

Fig. 7 Organic aerosol number concentration ($dN/d\log D_p$) plot as a function of size and time from the SMPS for two experiments conducted under air at 292 K and 438 ppbv of excess O_3. The top and bottom graphs differ only in the concentration of cashmeran used.

3.3.2 Particle phase. In addition to the gas phase measurements, we connected the scanning mobility particle sizer (SMPS) to the chamber to monitor the size and number concentrations of SOA during ozonolysis of cashmeran (see Section 2.3.2). We observed no significant particle formation in N_2 studies (Fig. S9†). However, particle formation under air was dependent on the concentration of cashmeran used, the temperature of the experiment, and the concentration of O_3.

To illustrate the dependence of SOA production on cashmeran concentrations, we compared two experiments conducted under air at the same temperature (292 K) and with excess O_3 (438 ppb), but with different cashmeran concentrations: 0.26 ppbv and 0.19 ppbv (Fig. 7). At 0.26 ppbv of cashmeran, we observed the onset of aerosol formation with a rapid increase in size and number concentrations. We calculated a number concentration of 3.24×10^6 #/cm^3 with total aerosol mass concentration of 3.82×10^2 μg m^{-3}. In contrast, no significant aerosol formation was observed at a lower cashmeran concentration of 0.19 ppb. The total particle number and mass concentrations measured were 1.40×10^5 #/cm^3 and 19.3 μg m^{-3}, respectively, at this lower concentration. The formation of SOA indoors from fragrant products has been observed in previous studies and was attributed to the presence of terpenes

like limonene.[75–78] However, our findings indicate that large compounds, like cashmeran, in these products could also affect the aerosol mass indoors.

Additionally, to minimize the formation of secondary organic aerosols (SOA), we determined the threshold mixing ratio for cashmeran at 292 K to be 0.19 ppbv. Above this concentration, we anticipate aerosol formation, as demonstrated in Fig. 7. Importantly, this concentration is lower than what we detected during the perfume analysis in Fig. 2. Thus, we demonstrate that the frequency and quantity of fragrant products used can impact indoor aerosol levels.

4 Atmospheric implication

We constrained the atmospheric fate of cashmeran, a dominant musk-smelling ingredient in perfumes, by investigating its fate against atmospheric oxidation. First, we determined the rate constant for the rate-limiting addition of O_3 to the C–C double bond in cashmeran to be $(2.78 \pm 0.31) \times 10^{-19}$ cm^3 molec^{-1} s^{-1} at ambient temperature in N_2. Cashmeran's lifetime in the presence of 20 ppbv of O_3, typical of indoor air,[61] would be 85 days. Moreover, the ozonolysis of cashmeran produced up to 5.1 $\times$ 10^5 molec cm^{-3} of OH radicals, a concentration comparable to typical steady-state levels indoors.[66] These OH radicals, in turn, oxidize cashmeran at much faster rates, leading to a lifetime of 5 h under the maximum OH concentrations of 5.1 $\times$ 10^5 molec cm^{-3} measured.

Furthermore, cashmeran will partition to surfaces, whether they be aerosols or indoor surfaces due to its low volatility, slow reactivity, and potential to form secondary organic aerosols. As a semi-volatile compound, we anticipate that cashmeran will sorb to the clothing and to diverse surfaces commonly found indoors, including carpets, upholstery, dust particles, and walls, after being emitted from a perfume.[79–82] Also, we expect the rate of sorption to the fabric on which it was applied to vary depending on the type of fabric and polarity of the molecule.[74,83] For example, as a polar molecule, cashmeran is likely to adsorb more readily to natural fibers like cotton and linen than to synthetic materials like polyester.[84] Similar to other semi-volatiles, cashmeran may then undergo heterogeneous surface chemistry with indoor oxidants like O_3 and OH radicals or re-volatilize into the gas phase.[74,85] Photodegradation may also play a role in determining the fate of this molecule, given its absorption at 320 nm (see Fig. S16†). Overall, taking typical indoor O_3 and OH radical concentrations, we would expect 99% of cashmeran's fate to be governed by OH radicals.

Importantly, we identify the ability of cashmeran, and likely of other alkene VCPs to generate secondary OH radicals during ozonolysis. The ozonolysis of cashmeran is slow due to the electron-poor double bond in the α,β-ketone, which results in a lower OH yield of 0.004% compared to electron-rich compounds like 1,3-butadiene (8%), cyclohexene (68%), propene (0.33%), α-pinene (76%), 2-butanol (70%), and 2,3-dimethyl-2-butene (100%). Yet, fragrant VCPs may still impact the oxidative capacity of indoor environments.[58,86,87] This yield of OH radicals from cashmeran ozonolysis decreases the lifetime of cashmeran by an order of magnitude (Fig. 8).

Finally, since cashmeran is relatively long-lived, it can spread throughout our environment (Table 1). Cashmeran is also a synthetic compound and is therefore indicative of anthropogenic activity. In addition, cashmeran is specifically emitted from fragrant personal care products. Based on this collective evidence, we propose that cashmeran, and likely similar musk compounds, are potential VCP tracers in urban air. Since cashmeran uniquely originates from perfumes, it can be added to the growing list of human-emitted chemical tracers like D5-siloxane in air quality studies.[2,88]

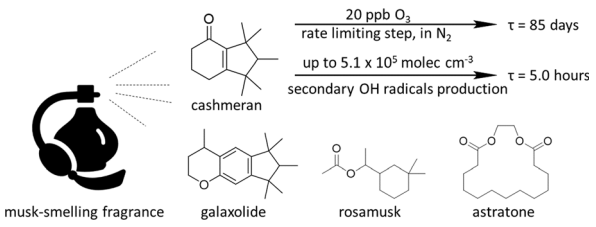

Fig. 8 The fate of cashmeran emitted from musk-smelling fragrances is depicted against O_3 and OH radicals produced during the reaction. Other compounds measured from the musk fragrance included galaxolide, rosamusk and astratone.

Data availability

Data presented in the figures of this study are available in the ESI† as a spreadsheet.

Conflicts of interest

There are no conflicts to declare.

Acknowledgements

We acknowledge the Canada Foundation for Innovation, BC Knowledge Development Fund, Alfred P. Sloan Foundation (#2020-13956), and the University of British Columbia for infrastructure and funding support. We thank Rickey Lee for his MATLAB code for the SMPS data. We also thank Benjamin Herring for help with the GC-MS analysis.

References

1 G. I. Gkatzelis, M. M. Coggon, B. C. McDonald, J. Peischl, J. B. Gilman, K. C. Aikin, *et al.*, Observations Confirm that Volatile Chemical Products Are a Major Source of Petrochemical Emissions in U.S. Cities, *Environ. Sci. Technol.*, 2021, **55**(8), 4332–4343, DOI: **10.1021/acs.est.0c05471**.

2 G. I. Gkatzelis, M. M. Coggon, B. C. McDonald, J. Peischl, K. C. Aikin, J. B. Gilman, *et al.*, Identifying Volatile Chemical Product Tracer Compounds in U.S. Cities, *Environ. Sci. Technol.*, 2021, **55**(1), 188–199, DOI: **10.1021/acs.est.0c05467**.

3 M. M. Coggon, G. I. Gkatzelis, B. C. McDonald, J. B. Gilman, R. H. Schwantes, N. Abuhassan, *et al.*, Volatile chemical product emissions enhance ozone and modulate urban chemistry, *Proc. Natl. Acad. Sci. U. S. A.*, 2021, **118**(32), e2026653118, DOI: **10.1073/pnas.2026653118**.

4 K. M. Seltzer, E. Pennington, V. Rao, B. N. Murphy, M. Strum, K. K. Isaacs, *et al.*, Reactive organic carbon emissions from volatile chemical products, *Atmos. Chem. Phys.*, 2021, **21**(6), 5079–5100, available from: **https://acp.copernicus.org/articles/21/5079/2021/**.

5 K. M. Seltzer, B. N. Murphy, E. A. Pennington, C. Allen, K. Talgo and H. O. T. Pye, Volatile Chemical Product Enhancements to Criteria Pollutants in the United States, *Environ. Sci. Technol.*, 2022, **56**(11), 6905–6913, DOI: **10.1021/acs.est.1c04298**.

6 M. Jerrett, R. T. Burnett, C. A. Pope, K. Ito, G. Thurston, D. Krewski, *et al.*, Long-Term Ozone Exposure and Mortality, *N. Engl. J. Med.*, 2009, **360**(11), 1085–1095, DOI: **10.1056/NEJMoa0803894**.

7 Canada H, *Volatile Organic Compounds*, 2017, last modified: 2021-01-15, available from: **https://www.canada.ca/en/health-canada/services/air-quality/indoor-air-contaminants/volatile-organic-compounds.html**.

8 K. Rumchev, H. Brown and J. Spickett, Volatile Organic Compounds: Do they present a risk to our health?, *Rev. Environ. Health*, 2007, **22**, 39–55.

9 A. M. Yeoman, M. Shaw, N. Carslaw, T. Murrells, N. Passant and A. C. Lewis, Simplified speciation and atmospheric volatile organic compound emission rates from non-aerosol personal care products, *Indoor Air*, 2020, **30**(3), 459–472.

10 X. Tang, P. K. Misztal, W. W. Nazaroff and A. H. Goldstein, Siloxanes Are the Most Abundant Volatile Organic Compound Emitted from Engineering Students in a Classroom, *Environ. Sci. Technol. Lett.*, 2015, **2**(11), 303–307, DOI: **10.1021/acs.estlett.5b00256**.

11 A. Steinemann, Volatile emissions from common consumer products, *Air Qual., Atmos. Health*, 2015, **8**(3), 273–281, DOI: **10.1007/s11869-015-0327-6**.

12 A. M. Peck and K. C. Hornbuckle, Synthetic musk fragrances in urban and rural air of Iowa and the Great Lakes, *Atmos. Environ.*, 2006, **40**(32), 6101–6111, available from: **https://www.sciencedirect.com/science/article/pii/S1352231006005188**.

13 Y. Lyu, S. Ren, F. Zhong, X. Han, Y. He and Z. Tang, Occurrence and trophic transfer of synthetic musks in the freshwater food web of a large subtropical lake, *Ecotoxicol. Environ. Saf.*, 2021, **213**, 112074, available from: **https://www.sciencedirect.com/science/article/pii/S0147651321001858**.

14 E. Balci, M. Genisoglu, S. C. Sofuoglu and A. Sofuoglu, Indoor air partitioning of Synthetic Musk Compounds: Gas, particulate matter, house dust, and window film, *Sci. Total Environ.*, 2020, **729**, 138798, available from: **https://www.sciencedirect.com/science/article/pii/S0048969720323159**.

15 F. Wong, M. Robson, L. Melymuk, C. Shunthirasingham, N. Alexandrou, M. Shoeib, *et al.*, Urban sources of synthetic musk compounds to the environment, *Environ. Sci.: Processes Impacts*, 2019, **21**(1), 74–88, available from: **https://pubs.rsc.org/en/content/articlelanding/2019/em/c8em00341f**.

16 C. J. Weschler and W. W. Nazaroff, Semivolatile organic compounds in indoor environments, *Atmos. Environ.*, 2008, **42**(40), 9018–9040, available from: **https://www.sciencedirect.com/science/article/pii/S1352231008008480**.

17 J. Liu, W. Zhang, Q. Zhou, Q. Zhou, Y. Zhang and L. Zhu, Polycyclic musks in the environment: A review of their concentrations and distribution, ecological effects and behavior, current concerns and future prospects, *Crit. Rev. Environ. Sci. Technol.*, 2021, **51**(4), 323–377, DOI: **10.1080/10643389.2020.1724748**.

18 V. Arruda, M. Simões and I. B. Gomes, Synthetic Musk Fragrances in Water Systems and Their Impact on Microbial Communities, *Water*, 2022, **14**(5), 692, available from: **https://www.proquest.com/docview/2637830447/abstract/83BE844CF6054F79PQ/1**.

19 D. Salvito, Synthetic Musk Compounds and Effects on Human Health?, *Environ. Health Perspect.*, 2005, **113**(12), A802, available from: **https://www.ncbi.nlm.nih.gov/pmc/articles/PMC1314954/**.

20 X. Li, Z. Chu, J. Yang, M. Li, M. Du, X. Zhao, *et al.*, Chapter Seven – Synthetic Musks: A Class of Commercial Fragrance Additives in Personal Care Products (PCPs) Causing Concern as Emerging Contaminants, *Vol. 81 of Emerging Pollutants and Their Effects on Marine Ecosystems*, ed. Chen B., Zhang B. H., Zhu Z. J. and Lee K., Academic Press, 2018. available from: **https://www.sciencedirect.com/science/article/pii/S0065288118300257**.

21 C. A. McDonough, P. A. Helm, D. Muir, G. Puggioni and R. Lohmann, Polycyclic Musks in the Air and Water of the Lower Great Lakes: Spatial Distribution and Volatilization from Surface Waters, *Environ. Sci. Technol.*, 2016, **50**(21), 11575–11583, DOI: **10.1021/acs.est.6b03657**.

22 C. Lange, B. Kuch and J. W. Metzger, Occurrence and fate of synthetic musk fragrances in a small German river, *J. Hazard. Mater.*, 2015, **282**, 34–40, available from: **https://www.sciencedirect.com/science/article/pii/S0304389414004841**.

23 L. Melymuk, M. Robson, S. A. Csiszar, P. A. Helm, G. Kaltenecker, S. Backus, *et al.*, From the City to the Lake: Loadings of PCBs, PBDEs, PAHs and PCMs from Toronto to Lake Ontario, *Environ. Sci. Technol.*, 2014, **48**(7), 3732–3741, DOI: **10.1021/es403209z**.

24 I. Weinberg, A. Dreyer and R. Ebinghaus, Waste water treatment plants as sources of polyfluorinated compounds, polybrominated diphenyl ethers and musk fragrances to ambient air, *Environ. Pollut.*, 2011, **159**(1), 125–132, available from: **https://www.sciencedirect.com/science/article/pii/S0269749110004288**.

25 H. P. Hutter, P. Wallner, H. Moshammer, W. Hartl, R. Sattelberger, G. Lorbeer, *et al.*, Blood concentrations of

polycyclic musks in healthy young adults, *Chemosphere*, 2005, **59**(4), 487–492, available from: https://www.sciencedirect.com/science/article/pii/S0045653505002158.

26 S. Eisenhardt, B. Runnebaum, K. Bauer and I. Gerhard, Nitromusk Compounds in Women with Gynecological and Endocrine Dysfunction, *Environ. Res.*, 2001, **87**(3), 123–130, available from: https://www.sciencedirect.com/science/article/pii/S0013935101943026.

27 K. Kannan, J. L. Reiner, S. H. Yun, E. E. Perrotta, L. Tao, B. Johnson-Restrepo, *et al.*, Polycyclic musk compounds in higher trophic level aquatic organisms and humans from the United States, *Chemosphere*, 2005, **61**(5), 693–700, available from: https://www.sciencedirect.com/science/article/pii/S0045653505004431.

28 H. Wang, J. Zhang, F. Gao, Y. Yang, H. Duan, Y. Wu, *et al.*, Simultaneous analysis of synthetic musks and triclosan in human breast milk by gas chromatography tandem mass spectrometry, *J. Chromatogr. B*, 2011, **879**(21), 1861–1869, available from: https://www.sciencedirect.com/science/article/pii/S1570023211003084.

29 M. Schlumpf, K. Kypke, M. Wittassek, J. Angerer, H. Mascher, D. Mascher, *et al.*, Exposure patterns of UV filters, fragrances, parabens, phthalates, organochlor pesticides, PBDEs, and PCBs in human milk: Correlation of UV filters with use of cosmetics, *Chemosphere*, 2010, **81**(10), 1171–1183, available from: https://www.sciencedirect.com/science/article/pii/S004565351001132X.

30 Z. Hu, Y. Shi, H. Niu and Y. Cai, Synthetic musk fragrances and heavy metals in snow samples of Beijing urban area, China, *Atmos. Res.*, 2012, **104–105**, 302–305, available from: https://www.sciencedirect.com/science/article/pii/S0169809511002870.

31 A. Sofuoglu, N. Kiymet, P. Kavcar and S. C. Sofuoglu, Polycyclic and nitro musks in indoor air: a primary school classroom and a women's sport center, *Indoor Air*, 2010, **20**(6), 515–522, DOI: 10.1111/j.1600-0668.2010.00674.x.

32 Y. Lu, T. Yuan, S. H. Yun, W. Wang and K. Kannan, Occurrence of Synthetic Musks in Indoor Dust from China and Implications for Human Exposure, *Arch. Environ. Contam. Toxicol.*, 2011, **60**(1), 182–189, DOI: 10.1007/s00244-010-9595-1.

33 H. Nakata, M. Hinosaka and H. Yanagimoto, Macrocyclic-, polycyclic-, and nitro musks in cosmetics, household commodities and indoor dusts collected from Japan: Implications for their human exposure, *Ecotoxicol. Environ. Saf.*, 2015, **111**, 248–255, available from: https://www.sciencedirect.com/science/article/pii/S0147651314004588.

34 I. T. I. Wang, S. F. Cheng and S. W. Tsai, Determinations of airborne synthetic musks by polyurethane foam coupled with triple quadrupole gas chromatography tandem mass spectrometer, *J. Chromatogr. A*, 2014, **1330**, 61–68, available from: https://www.sciencedirect.com/science/article/pii/S0021967314000533.

35 V. Homem, M. Llompart, M. Vila, A. R. L. Ribeiro, C. Garcia-Jares, N. Ratola, *et al.*, Gone with the flow - Assessment of personal care products in Portuguese rivers, *Chemosphere*, 2022, **293**, 133552, available from: https://www.sciencedirect.com/science/article/pii/S0045653522000418.

36 L. Trabalón, G. Cano-Sancho, E. Pocurull, M. Nadal, J. L. Domingo and F. Borrull, Exposure of the population of Catalonia (Spain) to musk fragrances through seafood consumption: Risk assessment, *Environ. Res.*, 2015, **143**, 116–122, available from: https://www.sciencedirect.com/science/article/pii/S0013935115001243.

37 F. Merhabi, E. Gomez, H. Amine, D. Rosain, J. Halwani and H. Fenet, Occurrence, distribution, and ecological risk assessment of emerging and legacy contaminants in the Kadicha river in Lebanon, *Environ. Sci. Pollut. Res.*, 2021, **28**(44), 62499–62518, DOI: 10.1007/s11356-021-15049-0.

38 K. Kannan, J. L. Reiner, S. Yun, E. Perrotta, L. Tao, B. Johnson-Restrepo, *et al.*, Polycyclic musk compounds in higher trophic level aquatic organisms and humans from the United States, *Chemosphere*, 2005, **61**(5), 693–700, available from: https://www.semanticscholar.org/paper/3b5eff30206e8c09b256f791bf339e2c70442834.

39 A. M. Api, D. Belsito, S. Biserta, D. Botelho, M. Bruze, G. A. Burton, *et al.*, RIFM fragrance ingredient safety assessment, 6,7-dihydro-1,1,2,3,3-pentamethyl-4(5H)-indanone, CAS Registry Number 33704-61-9, *Food Chem. Toxicol.*, 2021, **149**, 111929, available from: https://www.sciencedirect.com/science/article/pii/S027869152030819X.

40 Austrialian Industrial Chemicals Introdution Scheme, *Cashmeran (4H-Inden-4-One, 1,2,3,5,6,7-Hexahydro-1,1,2,3,3-Pentamethyl-)*, Evaluation Statement – 14, September, 2021.

41 S. Tayal, M. A. Schults, P. Sterchele, E. Hulzebos and G. S. Ladics, Cashmeran as a potential endocrine disrupting chemical: What does the weight-of-the-evidence indicate?, *Food Chem. Toxicol.*, 2024, **184**, 114351, available from: https://www.sciencedirect.com/science/article/pii/S0278691523007536.

42 R. J. M. Lee, A. A. Akande, P. A. Heine, P. Padihar, D. Tonkin, W. Rusinoff, C. Manke, D. Lovrity, T. Mittertreiner, M. A. Rezaei and N. Borduas-Dedekind, *The development of the UBC ATMOX chamber: An 8 m3 LED-powered wavelength-dependent modular environmental chamber for indoor and outdoor atmospheric chemistry*, to be submitted.

43 B. L. Deming, D. Pagonis, X. Liu, D. A. Day, R. Talukdar, J. E. Krechmer, *et al.*, Measurements of delays of gas-phase compounds in a wide variety of tubing materials due to gas–wall interactions, *Atmos. Meas. Tech.*, 2019, **12**(6), 3453–3461, available from: https://amt.copernicus.org/articles/12/3453/2019/.

44 D. Pagonis, J. E. Krechmer, J. de Gouw, J. L. Jimenez and P. J. Ziemann, Effects of gas–wall partitioning in Teflon tubing and instrumentation on time-resolved measurements of gas-phase organic compounds, *Atmos. Meas. Tech.*, 2017, **10**(12), 4687–4696, available from: https://amt.copernicus.org/articles/10/4687/2017/.

45 J. Krechmer, F. Lopez-Hilfiker, A. Koss, M. Hutterli, C. Stoermer, B. Deming, *et al.*, Evaluation of a New Reagent-Ion Source and Focusing Ion–Molecule Reactor for Use in Proton-Transfer-Reaction Mass Spectrometry, *Anal. Chem.*, 2018, **90**(20), 12011–12018, DOI: **10.1021/acs.analchem.8b02641**.

46 H. Li, T. G. Almeida, Y. Luo, J. Zhao, B. B. Palm, C. D. Daub, *et al.*, Fragmentation inside proton-transfer-reaction-based mass spectrometers limits the detection of ROOR and ROOH peroxides, *Atmos. Meas. Tech.*, 2022, **15**(6), 1811–1827, available from: **https://amt.copernicus.org/articles/15/1811/2022/**.

47 T. Reinecke, M. Leiminger, A. Jordan, A. Wisthaler and M. Müller, Ultrahigh Sensitivity PTR-MS Instrument with a Well-Defined Ion Chemistry, *Anal. Chem.*, 2023, **95**(32), 11879–11884, DOI: **10.1021/acs.analchem.3c02669**.

48 K. Sekimoto, S. M. Li, B. Yuan, A. Koss, M. Coggon, C. Warneke, *et al.*, Calculation of the sensitivity of proton-transfer-reaction mass spectrometry (PTR-MS) for organic trace gases using molecular properties, *Int. J. Mass Spectrom.*, 2017, **421**, 71–94, available from: **https://www.sciencedirect.com/science/article/pii/S1387380616302494**.

49 M. D. Keywood, J. H. Kroll, V. Varutbangkul, R. Bahreini, R. C. Flagan and J. H. Seinfeld, Secondary Organic Aerosol Formation from Cyclohexene Ozonolysis: Effect of OH Scavenger and the Role of Radical Chemistry, *Environ. Sci. Technol.*, 2004, **38**(12), 3343–3350, DOI: **10.1021/es049725j**.

50 EPA U and US EPA, *Estimation Programs Interface Suite™ for Microsoft® Windows, V 11*, United States Environmental Protection Agency, Washington, DC, USA, 2024.

51 R. Atkinson, Kinetics and mechanisms of the gas-phase reactions of the hydroxyl radical with organic compounds under atmospheric conditions, *Chem. Rev.*, 1986, **86**(1), 69–201, DOI: **10.1021/cr00071a004**.

52 B. Bohn and C. Zetzsch, Kinetics and mechanism of the reaction of OH with the trimethylbenzenes – experimental evidence for the formation of adduct isomers, *Phys. Chem. Chem. Phys.*, 2012, **14**(40), 13933–13948, available from: **https://pubs.rsc.org/en/content/articlelanding/2012/cp/c2cp42434g**.

53 C. T. Pate, R. Atkinson and J. N. Pitts Jr, The gas phase reaction of O_3 with a series of aromatic hydrocarbons, *J. Environ. Sci. Health, Part A: Environ. Sci. Eng.*, 1976, **11**(1), 1–10, DOI: **10.1080/10934527609385750**.

54 F. Kramp and S. E. Paulson, On the Uncertainties in the Rate Coefficients for OH Reactions with Hydrocarbons, and the Rate Coefficients of the 1,3,5-Trimethylbenzene and m-Xylene Reactions with OH Radicals in the Gas Phase, *J. Phys. Chem. A*, 1998, **102**(16), 2685–2690, DOI: **10.1021/jp973289o**.

55 S. E. Paulson, J. D. Fenske, A. D. Sen and T. W. Callahan, A Novel Small-Ratio Relative-Rate Technique for Measuring OH Formation Yields from the Reactions of O_3 with Alkenes in the Gas Phase, and Its Application to the Reactions of Ethene and Propene, *J. Phys. Chem. A*, 1999, **103**(13), 2050–2059, DOI: **10.1021/jp984140v**.

56 A. C. Steinemann, Fragranced consumer products and undisclosed ingredients, *Environ. Impact Assess. Rev.*, 2009, **29**(1), 32–38, available from: **https://www.sciencedirect.com/science/article/pii/S0195925508000899**.

57 S. E. Paulson and J. J. Orlando, The reactions of ozone with alkenes: An important source of HOx in the boundary layer, *Geophys. Res. Lett.*, 1996, **23**(25), 3727–3730, DOI: **10.1029/96GL03477**.

58 R. Atkinson and S. M. Aschmann, Hydroxyl radical production from the gas-phase reactions of ozone with a series of alkenes under atmospheric conditions, *Environ. Sci. Technol.*, 1993, **27**(7), 1357–1363, DOI: **10.1021/es00044a010**.

59 D. K. Farmer, M. E. Vance, J. P. D. Abbatt, A. Abeleira, M. R. Alves, C. Arata, *et al.*, Overview of HOMEChem: House Observations of Microbial and Environmental Chemistry, *Environ. Sci.: Processes Impacts*, 2019, **21**(8), 1280–1300, available from: **http://xlink.rsc.org/?DOI=C9EM00228F**.

60 D. K. Farmer, M. E. Vance, D. Poppendieck, J. Abbatt, M. R. Alves, K. C. Dannemiller, *et al.*, The chemical assessment of surfaces and air (CASA) study: using chemical and physical perturbations in a test house to investigate indoor processes, *Environ. Sci.: Processes Impacts*, 2024, DOI: **10.1039/d4em00209a**, available from: **https://pubs.rsc.org/en/content/articlelanding/2024/em/d4em00209a**.

61 Canada H, *Residential Indoor Air Quality Guidelines [education and Awareness]*, 2015, **https://www.canada.ca/en/health-canada/services/air-quality/residential-indoor-air-quality-guidelines.html**.

62 Z. Zhao, W. Zhang, T. Alexander, X. Zhang, D. B. C. Martin and H. Zhang, Isolating α -Pinene Ozonolysis Pathways Reveals New Insights into Peroxy Radical Chemistry and Secondary Organic Aerosol Formation, *Environ. Sci. Technol.*, 2021, **55**(10), 6700–6709, DOI: **10.1021/acs.est.1c02107**.

63 M. Siese, K. H. Becker, K. J. Brockmann, H. Geiger, A. Hofzumahaus, F. Holland, *et al.*, Direct Measurement of OH Radicals from Ozonolysis of Selected Alkenes: A EUPHORE Simulation Chamber Study, *Environ. Sci. Technol.*, 2001, **35**(23), 4660–4667, DOI: **10.1021/es010150p**.

64 K. S. Docherty and P. J. Ziemann, Effects of Stabilized Criegee Intermediate and OH Radical Scavengers on Aerosol Formation from Reactions of β -Pinene with O_3, *Aerosol Sci. Technol.*, 2003, **37**(11), 877–891, DOI: **10.1080/02786820300930**.

65 S. M. Aschmann, A. A. Chew, J. Arey and R. Atkinson, Products of the Gas-Phase Reaction of OH Radicals with Cyclohexane: Reactions of the Cyclohexoxy Radical, *J. Phys. Chem. A*, 1997, **101**(43), 8042–8048, DOI: **10.1021/jp971869f**.

66 C. J. Weschler and H. C. Shields, Production of the Hydroxyl Radical in Indoor Air, *Environ. Sci. Technol.*, 1996, **30**(11), 3250–3258, DOI: **10.1021/es960032f**.

67 E. Gomez Alvarez, D. Amedro, C. Afif, S. Gligorovski, C. Schoemaecker, C. Fittschen, *et al.*, Unexpectedly high

indoor hydroxyl radical concentrations associated with nitrous acid, *Proc. Natl. Acad. Sci. U. S. A.*, 2013, **110**(33), 13294–13299, DOI: 10.1073/pnas.1308310110.

68 M. R. McGillen, C. J. Percival, D. E. Shallcross and J. N. Harvey, Is hydrogen abstraction an important pathway in the reaction of alkenes with the OH radical?, *Phys. Chem. Chem. Phys.*, 2007, **9**(31), 4349–4356, available from: https://pubs.rsc.org/en/content/articlelanding/2007/cp/b703035e.

69 Q. D. Wang, M. M. Sun and J. H. Liang, Reaction Mechanisms and Kinetics of the Hydrogen Abstraction Reactions of C4–C6 Alkenes with Hydroxyl Radical: A Theoretical Exploration, *Int. J. Mol. Sci.*, 2019, **20**(6), 1275, available from: https://www.ncbi.nlm.nih.gov/pmc/articles/PMC6471405/.

70 Z. Tian, Y. Liu, J. Li and Y. Yan, Theoretical study of H-abstraction and addition reactions of cyclohexene with H, OH and HO_2, *Fuel*, 2023, **332**, 125891, available from: https://www.sciencedirect.com/science/article/pii/S0016236122027156.

71 D. Johnson and G. Marston, The gas-phase ozonolysis of unsaturated volatile organic compounds in the troposphere, *Chem. Soc. Rev.*, 2008, **37**(4), 699–716, available from: https://pubs.rsc.org/en/content/articlelanding/2008/cs/b704260b.

72 S. A. Epstein and N. M. Donahue, The Kinetics of Tetramethylethene Ozonolysis: Decomposition of the Primary Ozonide and Subsequent Product Formation in the Condensed Phase, *J. Phys. Chem. A*, 2008, **112**(51), 13535–13541, DOI: 10.1021/jp807682y.

73 R. Chhantyal-Pun, M. A. H. Khan, C. A. Taatjes, C. J. Percival, A. J. Orr-Ewing and D. E. Shallcross, Criegee intermediates: production, detection and reactivity, *Int. Rev. Phys. Chem.*, 2020, **39**(3), 385–424, DOI: 10.1080/0144235X.2020.1792104.

74 A. D. L. Wylie and J. P. D. Abbatt, Heterogeneous Ozonolysis of Tetrahydrocannabinol: Implications for Thirdhand Cannabis Smoke, *Environ. Sci. Technol.*, 2020, **54**(22), 14215–14223, DOI: 10.1021/acs.est.0c03728.

75 S. Rossignol, C. Rio, A. Ustache, S. Fable, J. Nicolle, A. Même, *et al.*, The use of a housecleaning product in an indoor environment leading to oxygenated polar compounds and SOA formation: Gas and particulate phase chemical characterization, *Atmos. Environ.*, 2013, **75**, 196–205, available from: https://www.sciencedirect.com/science/article/pii/S1352231013002215.

76 G. Sarwar, D. A. Olson, R. L. Corsi and C. J. Weschler, Indoor Fine Particles: The Role of Terpene Emissions from Consumer Products, *J. Air Waste Manage. Assoc.*, 2004, **54**(3), 367–377, DOI: 10.1080/10473289.2004.10470910.

77 C. M. F. Rosales, J. Jiang, A. Lahib, B. P. Bottorff, E. K. Reidy, V. Kumar, *et al.*, Chemistry and human exposure implications of secondary organic aerosol production from indoor terpene ozonolysis, *Sci. Adv.*, 2022, **8**(8), eabj9156, DOI: 10.1126/sciadv.abj9156.

78 T. Wu, T. Müller, N. Wang, J. Byron, S. Langer, J. Williams, *et al.*, Indoor Emission, Oxidation, and New Particle Formation of Personal Care Product Related Volatile Organic Compounds, *Environ. Sci. Technol. Lett.*, 2024, **11**(10), 1053–1061, DOI: 10.1021/acs.estlett.4c00353.

79 J. P. D. Abbatt and C. Wang, The atmospheric chemistry of indoor environments, *Environ. Sci.: Processes Impacts*, 2020, **22**(1), 25–48, available from: https://pubs.rsc.org/en/content/articlelanding/2020/em/c9em00386j.

80 R. B. Jørgensen, O. Bjørseth and B. Malvik, Chamber testing of adsorption of volatile organic compounds (VOCs) on material surfaces, *Indoor Air*, 1999, **9**(1), 2–9.

81 N. Borduas, J. G. Murphy, C. Wang, G. da Silva and J. P. D. Abbatt, Gas Phase Oxidation of Nicotine by OH Radicals: Kinetics, Mechanisms, and Formation of HNCO, *Environ. Sci. Technol. Lett.*, 2016, **3**(9), 327–331, DOI: 10.1021/acs.estlett.6b00231.

82 B. A. Tichenor, Z. Guo, J. E. Dunn, L. E. Sparks and M. A. Mason, The Interaction of Vapour Phase Organic Compounds with Indoor Sinks, *Indoor Air*, 1991, **1**(1), 23–35, DOI: 10.1111/j.1600-0668.1991.03-11.x.

83 J. Yu, F. Wania and J. P. D. Abbatt, A New Approach to Characterizing the Partitioning of Volatile Organic Compounds to Cotton Fabric, *Environ. Sci. Technol.*, 2022, **56**(6), 3365–3374, DOI: 10.1021/acs.est.1c08239.

84 A. Saini, J. O. Okeme, J. Mark Parnis, R. H. McQueen and M. L. Diamond, From air to clothing: characterizing the accumulation of semi-volatile organic compounds to fabrics in indoor environments, *Indoor Air*, 2017, **27**(3), 631–641, DOI: 10.1111/ina.12328.

85 K. Yeh, L. Li, F. Wania and J. P. D. Abbatt, Thirdhand smoke from tobacco, e-cigarettes, cannabis, methamphetamine and cocaine: Partitioning, reactive fate, and human exposure in indoor environments, *Environ. Int.*, 2022, **160**, 107063, available from: https://www.sciencedirect.com/science/article/pii/S0160412021006887.

86 G. E. Orzechowska and S. E. Paulson, Production of OH radicals from the reactions of C4–C6 internal alkenes and styrenes with ozone in the gas phase, *Atmos. Environ.*, 2002, **36**(3), 571–581, available from: https://www.sciencedirect.com/science/article/pii/S1352231001004459.

87 A. A. Chew and R. Atkinson, OH radical formation yields from the gas-phase reactions of O3 with alkenes and monoterpenes, *J. Geophys. Res.: Atmos.*, 1996, **101**(D22), 28649–28653, DOI: 10.1029/96JD02722.

88 L. H. Rivellini, S. Jorga, Y. Wang, A. K. Y. Lee, J. G. Murphy, A. W. Chan, *et al.*, Sources of Wintertime Atmospheric Organic Pollutants in a Large Canadian City: Insights from Particle and Gas Phase Measurements, *ACS ES&T Air*, 2024, **1**(7), 690–703, DOI: 10.1021/acsestair.4c00039.

